Laser surface treatment of polyamide and NiTi alloy and the effects on mesenchymal stem cell response

D.G. Waugh[1], J. Lawrence[1], P. Shukla[1], C. Chan[2], I. Hussain[3], H.C. Man[4], G.C. Smith[1]

[1]Laser Engineering and Manufacturing Research Group, Faculty of Science and Engineering, University of Chester, Thornton Science Park, Pool Lane, Ince, Chester CH2 4NU, UK
[2]School of Mechanical and Aerospace Engineering, Queen's University Belfast, Northern Ireland, UK
[3]School of Life Sciences, University of Lincoln, Brayford Pool, Lincoln, LN6 7TU, UK
[4] Department of Industrial and Systems Engineering, The Hong Kong Polytechnic University, Hung Hom, Kowloon, Hong Kong, China

Abstract

Mesenchymal stem cells (MSCs) are known to play important roles in development, post-natal growth, repair, and regeneration of mesenchymal tissues. What is more, surface treatments are widely reported to affect the biomimetic nature of materials. This paper will detail, discuss and compare laser surface treatment of polyamide (Polyamide 6,6), using a 60 W CO_2 laser, and NiTi alloy, using a 100 W fiber laser, and the effects of these treatments on mesenchymal stem cell response. The surface morphology and composition of the polyamide and NiTi alloy were studied by scanning electron microscopy (SEM) and X-ray photoemission spectroscopy (XPS), respectively. MSC cell morphology cell counting and viability measurements were done by employing a haemocytometer and MTT colorimetric assay. The success of enhanced adhesion and spreading of the MSCs on each of the laser surface treated samples, when compared to as-received samples, is evidenced in this work.

Keywords: stem cells, laser surface treatment, CO_2 laser, fiber laser, MTT, cell viability.

1. Introduction

In the last 10 years the biological applications of polymers and alloys has significantly increased. For instance, polyamide can be utilized within the biomaterial industry as sutures [1], vascular grafts [2] and other hard tissue implants [3]. NiTi alloys have been widely used for bio-medical applications such as cardiovascular, orthopedic and dental applications [4-6]. NiTi alloys have also been used for the manufacture of advanced surgical instruments because of the shape-memory effect (SME), superelasticity (SE) and fairly good biocompatibility [7, 8].

By extrapolating from past and current research it is imperative that any biomaterial should be optimized in order for that material to function appropriately and efficiently within the desired biological environment. In numerous instances it is seen that the bulk properties of a biomaterial are decided upon such that the surface properties are compromised. In particular, this is seen throughout the use of polymeric biomaterials as they offer excellent bulk properties for biological applications; however, the surface properties they possess do not lend themselves to high performance in regards to biomimetics [9]. On account of this, it is necessary to vary the surface properties of the material without hindering the bulk properties in order to enhance the wettability and bioactivity. In terms of bioactivity a biomaterial can be surface modified both topographically and chemically in order to manipulate the way in which the cells react.

Owing to the unique shape memory and super-elastic effects (SME and SE), and apparent biocompatibility, NiTi has become an important bio-material for orthopaedic applications in the last decade [7]. Also, due to the increasing demand in miniaturization of medical implants, laser micro-welding has been treated as the most promising joining technique in the clinical and medical device industry by virtue of its capability to deliver the advantages of high precision with small and localized heat input [10].

The interaction between cells and biomaterial is considered as an essential indication for the biocompatibility, and such interaction is often affected by a list of surface properties, such as surface roughness, topography, chemistry and hydrophilicity. Curtis *et al.* [11] stated that cells are able to discriminate among subtle differences in surface roughness and topography, resulting in different protein adsorption and cellular responses of morphology, differentiation, proliferation, and orientation. The degree of responses is varying from one type of cell to another. Generally, osteoblasts prefer rough surfaces while fibroblast cells prefer smooth surfaces [12, 13]. Previous studies with the MSCs performed on materials indicate that MSCs are sensitive to the surface roughness and topography. Kommireddy *et al.* [14] reported cell attachment of MSCs is affected by the surface roughness and increased cell attachment is found on the rougher surface than the smoother surfaces. In addition to this Myllymaa *et al.* [15] found that MSCs are sensitive to the topographical variations and are likely to interact with the physical environment by aligning their orientation along the physical shape and edges.

On account of the importance and increase in research in to biomedical applications of polymeric materials and alloys, this work details the laser surface treatment of polyamide and NiTi alloy, comparing the bioactivity of these materials with respect to stem cell growth response following the surface treatment.

2. Experimental Technique

2.1 Materials

The polyamide 6,6 was sourced in 100×100 mm^2 sheets with a thickness of 5 mm (Goodfellow Cambridge, Ltd). To obtain a conveniently sized sample for experimentation the as-received polyamide sheet was cut into 30 mm diameter discs using a 1 kW continuous wave (cw) CO_2 laser (Everlase S48; Coherent, Ltd).

The NiTi was flat annealed Ti–55.91 wt.% Ni foil in the form of 50×50×0.25 mm (Johnson Matthey, Inc.). It was ground using SiC papers of 600 grit to remove oxide scales on the sample surface. The samples were ultrasonically degreased in pure alcohol for 10 min, followed by 5 min of cleaning in distilled water, and dried thoroughly in air before laser welding.

2.2 Laser Processing of Polyamide

In order to generate the required marking pattern with the 10.6 μm CO_2 laser system (60W, Firestar-Ti; Synrad, Inc.) Winmark software version 2.1.0, build 3468 was used. In addition, the software was capable of using images saved as .dxf files which can be produced by using CAD programs such as, in this case, Licom AutoCaM. The polyamide 6,6 samples where placed into the laser system onto a stage in which they where held in place using a bracket with a 30.5 mm diameter hole cut into the centre of the bracket. The surface of the sample was set to be 250 mm away from the output facet of the laser system to obtain focus and the system utilized a galvanometer scanner to scan the 95 μm spot size beam directly across the stationary target material. It should be noted that the target material and laser system was held in a laser safety cabinet in which the ambient gas was air and an extraction system was used to remove any fumes produced during laser processing.

There were four patterns induced onto the surfaces of the polyamide 6,6 samples which were trenches with 50 μm spacing (CT50), hatch with 50 μm spacing (CH50), trenches with 100 μm spacing (CT100) and hatch with 100 μm spacing (CH100). In addition, an as-received control sample was used (AR). For each of the irradiated patterns the laser power was set to 12% (7 W) operating at 600 mms^{-1}.

2.3 Laser Processing of NiTi Alloy

A 100-W continuous wave (CW) fiber laser (SP-100C-0013; SPI and A&P Co., Ltd.) with a wavelength of 1091 nm was used for the melting. A x–y–z multistage manipulator (or welding jig) was used to adjust the samples in an appropriate position, and to apply a clamping force to the samples for minimizing thermal distortion. Argon was used as the shielding gas to suppress the formation of plasma in the vapor over the melt zone by blowing them away and to prevent the samples from oxidizing during laser melting. The Ar gas was delivered via the laser nozzle (central jet) of 10 mm in diameter and a copper pipe (side jet) of 6 mm in diameter to the melt zone. The side jet was tilted a 30° to the horizontal plane. The gas flow rate was controlled by a flow meter. The optimized parameters of laser power, speed, focus position, gas flow rate,

and shielding environment were: 70 W, 300 mm/min, +1.6 mm (away from the top surface of samples), 35 l/min and under Ar shielding. An as-received control sample (BM) was also used to compare between the base material and the laser surface treated samples.

2.4 Topography and Surface Chemistry Analysis

The surface profiles were determined using a white light interferometer (WLI) (NewView 500; Zygo, Ltd.). The WLI was set-up using a ×50 Mirau lens (NA=0.55) with working distance of 3.4 mm. The Ra and maximum peak-to-valley height roughness parameters for each sample were determined using the MetroPro Software, where Ra can be defined as the arithmetic average of the absolute values along a single specified direction. The mean and experimental standard deviation of parameters were obtained from five measurements.

For the polyamide, samples were analysed using x-ray photoelectron spectroscopy (XPS). This allowed any surface modifications in terms of surface oxygen content due to the laser irradiation to be revealed. The XPS data were acquired using a bespoke ultra-high vacuum system fitted with a Specs GmbH Focus 500 monochromated Al Kα X-ray source, Specs GmbH Phoibos 150 mm mean radius hemispherical analyser with 9-channeltron detection, and a Specs GmbH FG20 charge neutralising electron gun.

For the NiTi, the compositions at the surface without sputter cleaning were also analysed using XPS (PHI5600, Physical Electronics, Inc.) with a take-off angle of 45° normal to the sample surface. The X-ray source was monochromatic Al K alpha (15 kV, 25 W) and the beam size was 100 μm in diameter. The pass energy for survey scan and narrow scan spectra were 187.5 and 58.7 eV, respectively.

2.5 *In Vitro* Experimentation

A research laboratory safety protocol was followed. To avoid contamination of the cells, the culture work was conducted within a Class II Microbiological Safety Cabinet, and sterile conditions were maintained. The Mesenchymal stem cells (Stem Cell Bank, Japan) were grown in tissue culture medium consisting of DMEM (with L-glutamine) (Sigma Aldrich, Ltd.), supplemented with 10% foetal calf serum (FCS) (Sigma Aldrich, Ltd.), and 100 units/ml of penicillin/and 0.1- mg/ml of streptomycin (Sigma Aldrich, Ltd.), and placed in an incubator set at 37 °C, 5 % humidified CO2 (Wolf Laboratories, Ltd.), throughout the study. When the cells reached subconfluent (70 to 80 %), they were retrieved with 0.25 % trypsin and 0.02 % EDTA. The retrieved cells were washed twice with PBS, centrifuged at 1200 rpm for 12 minutes at room temperature and re-seeded into two 24-well plates cell culture at the initial seeding density of 5 × 104 cells per well. The two well plates were then placed in the incubator for times between 24 hours (1 day) and 96 hours (4 days).

3. Results and Discussion

3.1 Topography

3.1.1 Polyamide

Qualitatively the laser irradiated polyamide 6,6 samples were considerably rougher in comparison to the as-received reference control sample. It was possible to ascertain that the resulting surface pattern was more defined in one axis of the hatch in comparison to the other. This is a resultant of the way in which the CO_2 laser marker scanned the input image onto the target sample.

The roughness for each of the laser surface treated polyamide surfaces had increased and slight periodicity in the laser patterned samples was seen in contrast to the as-received sample (AR). In comparison to the as-received sample (AR), which had peak heights of the order of 0.1 to 0.2 μm, the peak heights for all of the laser treated samples were around 1 μm. It was also observed that the least periodicity arose from those samples which had patterns with 50 μm spacings . This can be seen to be of some importance as the laser spot size at the surface of the target samples was 95 μm consequently allowing the scans for the trenches and hatch patterns to overlap and ultimately eliminate the natural periodicity of the

original scanned pattern. However, the scan overlap occurring did ensure that the whole of the surface of the target sample was irradiated and modified in comparison to the non-irradiated reference sample (AR).

3.1.2 NiTi

Figure 1 (a-c) shows the surface morphology of the laser melt in the three regions: melt zone: MZ, heat affected zone: HAZ, and as-received base material: BM. Figure 1 (d) gives the morphology of the MZ after polishing. From Figure 1 (a), a typical tree-like or dendritic pattern arose as a result of rapid solidification of grains along the energetically favourable crystallographic direction in laser melting can be seen in the MZ. The morphology of the HAZ and BM was similar as evidenced from Figure 1 (b-c) and exhibited some surface defects, such as pores and grooves, which came from the manufacturing processes. For the MZ (ground), obvious grooves as a result of mechanical grinding by sandpaper were clearly found on the sample surface. No visible grooves were observed from the MZ (polished) as given in Figure 1 (d).

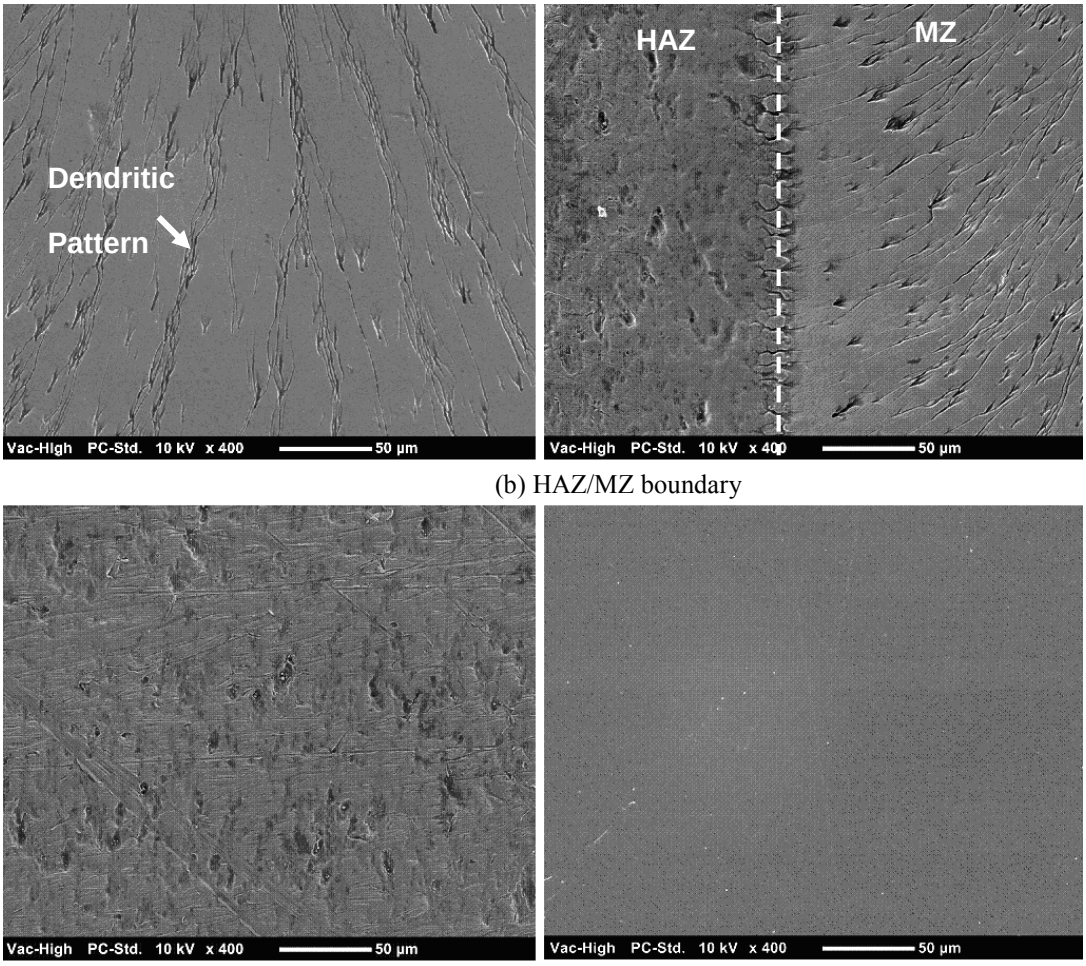

(a) MZ (b) HAZ/MZ boundary

(c) BM (d) MZ (polished)

Figure 1: SEM morphology of different samples

White Light Interferometry (WLI) was employed to obtain the roughness parameters of the samples and allowed for the surface profiles to be investigated. The Ra and maximum peak-to-valley height of the MZ was 0.375 ± 0.038 µm and 2.49 ± 0.314 µm respectively. Compared with the MZ, a relative smoother surface was observed with the HAZ and BM as evidenced by the smaller Ra and maximum peak-to-valley height. The dendritic pattern caused by the rapid cooling effect

of laser melting induced a roughening effect in the MZ compared to the HAZ and BM, while the grain growth effect in the HAZ did not cause any observable changes in the surface roughness, as evidenced by the similar Ra and maximum peak-to-valley height to the BM. In contrast to the MZ, the MZ (ground) showed completely different topography with smaller maximum peak-to-valley height of 1.67 ± 0.243 μm, though their Ra was similar. The MZ (polished) showed a smoother surface as compared to that of the MZ. The Ra of the MZ (polished) was 0.017 ± 0.006 μm and the maximum peak-to-valley height was 0.14 ± 0.039 μm.

3.2 Surface Composition

3.2.1 Polyamide

Results show that the laser treatment gave rise to a small increase in the oxygen and reduction in carbon compared to the AR sample, and a substantial increase in the nitrogen along with reductions in sodium and sulfur. The ideal form reference data (with peaks 1 and 2 added in intensity) would be 67% C-C, 17% C-N and 17% C=O. All treated samples except the CH50 are very close to this, with some very low intensity surface acid groups also found on CT50 and CH100.

As for the carbon spectra, all oxygen spectra from the laser-treated samples were very similar, but different from the AR reference sample. The AR sample showed a main component at ~ 531.5 eV attributed to C=O in polyamide (as expected) with a weaker but still significant component at ~533.1 eV attributed to oxygen in acid groups.

A ~533 eV component was identified which was not expected from the pure polyamide reference. Its persistence indicates the presence of possible C-O or surface acid groups on all treated samples. All samples showed a main nitrogen 1s peak at 399.6 – 399.8 eV binding energy, consistent with the reference data for nitrogen in C-N bonds in nylon. For most samples, this was the only component detected. However, the CH50 sample also showed some evidence for the presence of an additional very weak nitrogen 1s component at ~ 398.4 eV (~4% of total nitrogen 1s intensity). This component does not correspond well with reliable reference data from stoichiometric polymers, but is consistent with some early data on C=N bond configurations.

3.2.2 NiTi

The surface element of the samples was composed of carbon, oxygen, nitrogen, titanium, and nickel. Two peaks at 458.4 and 464.2 eV were identified as Ti $2p_{3/2}$ and Ti $2p_{1/2}$ respectively, and correspond to the presence of Ti^{4+} which is responsible for the TiO_2 formation. The results from the survey scan and the narrow scan for Ti 2_P region suggested that the major component of the outermost surface layer of the samples were TiO_2, with some other Ti sub-oxides and intermediate NiTi. The presence of carbon and nitrogen can be attributed to the surface contamination from the environment. The surface Ti/Ni ratio of the MZ was determined as 10.4 and is higher than that found in the HAZ and BM; namely 6.8 and 5.5, respectively.

3.3 Stem Cell Bioactivity

3.3.1 Polyamide

It can be seen from Figure 2, for the polyamide samples, that the number of mesenchymal stem cells increased over time, especially in the presence of the laser surface treated polyamide samples. The manner of reaction seen in the cells themselves was variable depending on the processing parameters used. The 24 hour results were generally lower than those seen at the longer incubations. This is due to the fact that when cells are seeded onto a surface, the cells go through a lag phase before entering the growth phase. In the vast majority of samples all readings were higher than those found in the AR control sample, as well as this, incubation over time also yielded higher readings. It should be noted that the highest

cell count ($183x10^3$) was recorded following 4 days incubation for the CH50 sample and could be due to this particular sample having the largest variation is surface chemistry composition. The lowest cell count ($100x10^3$) arose on the AR control sample following 24 hours of incubation and also had the lowest increase in cell number during the 3 day incubation with a cell number of $105x10^3$ after 4 days incubation. This highlights that the laser surface treatment of the polyamide samples significantly augmented the mesenchymal stem cell growth when compared to the AR control sample.

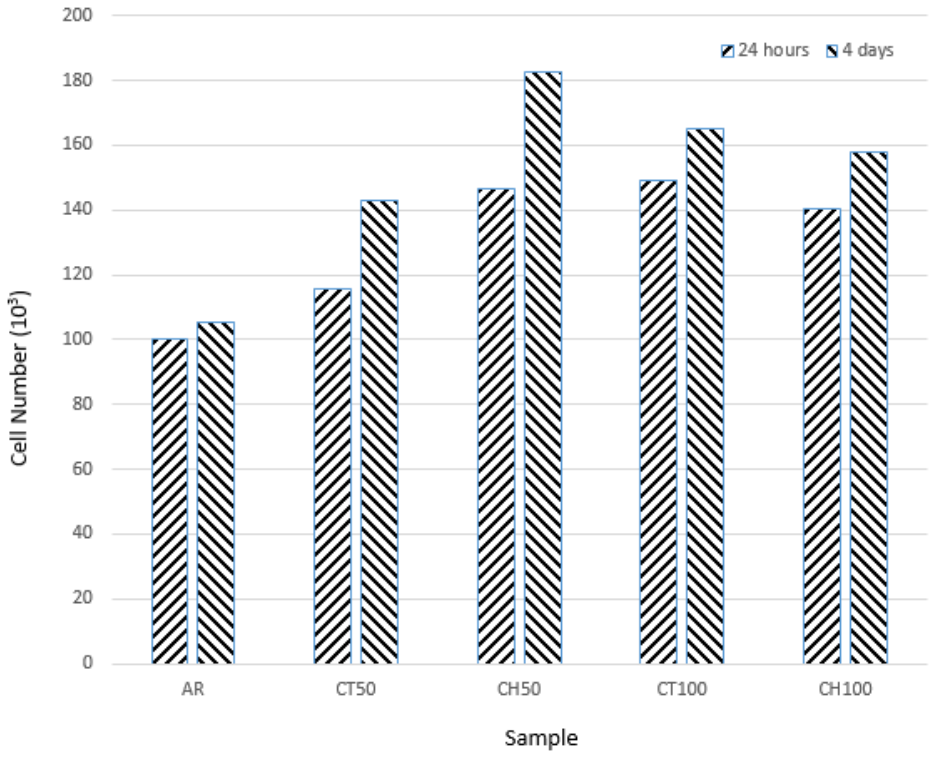

Figure 2: Stem cell count for each polyamide sample.

The cells grown on the AR control samples grew noticeably over 48 hours as opposed to 24 hours; it is also of note that all samples that were grown on polyamide samples grew much better than the blanks which were grown in the absence of nylon. The laser treated samples all grew better than their as received counterpart. Absorbance was noted to be highest under the CH50 sub group, in this group the 48 hour absorbance was higher than the 24 hour a theme that was repeated in both the blank, AR and CT100 group. In the CT50 and the CH100 group the 24 hour absorbance was slightly higher than the 48 hour absorbance; however the values received were close in both these groups.

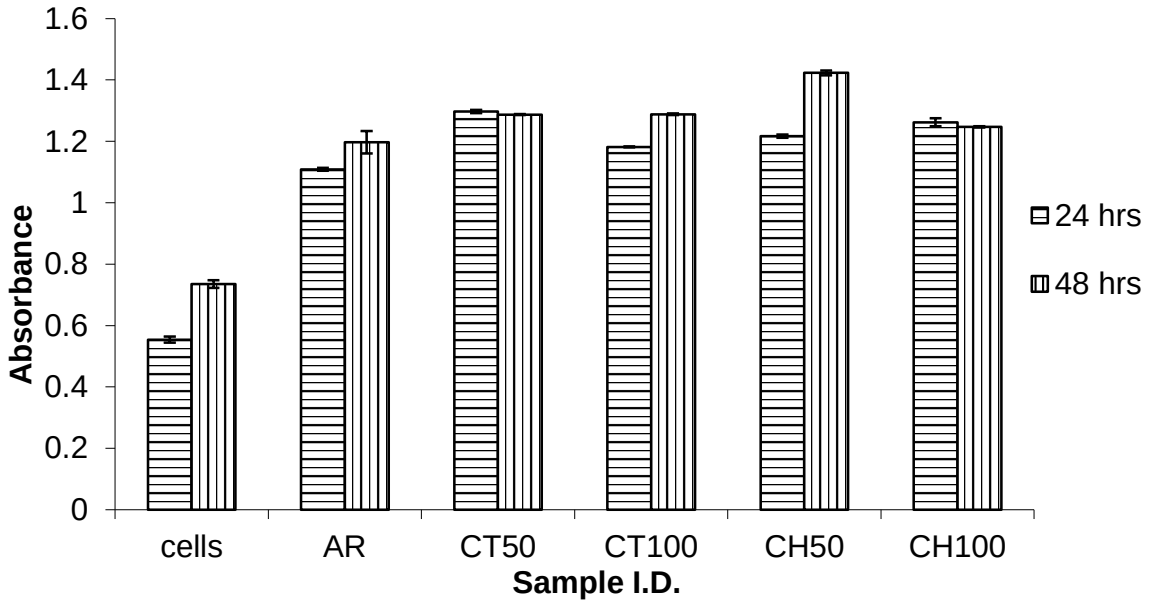

Figure 3: Viability MTT absorbance results for each polyamide sample.

3.3.2 NiTi

The number of viable cells on different samples after 1 and 4 days of culture is plotted in Figure 4. From the results, MZ (as-treated) shows a higher number of cells compared with MZ (polished) and HAZ for all culture periods and the BM after 4 days of culture. It should be noted that the cell number was less for the HAZ following 1 day and 4 day incubation times when compared to the BM.

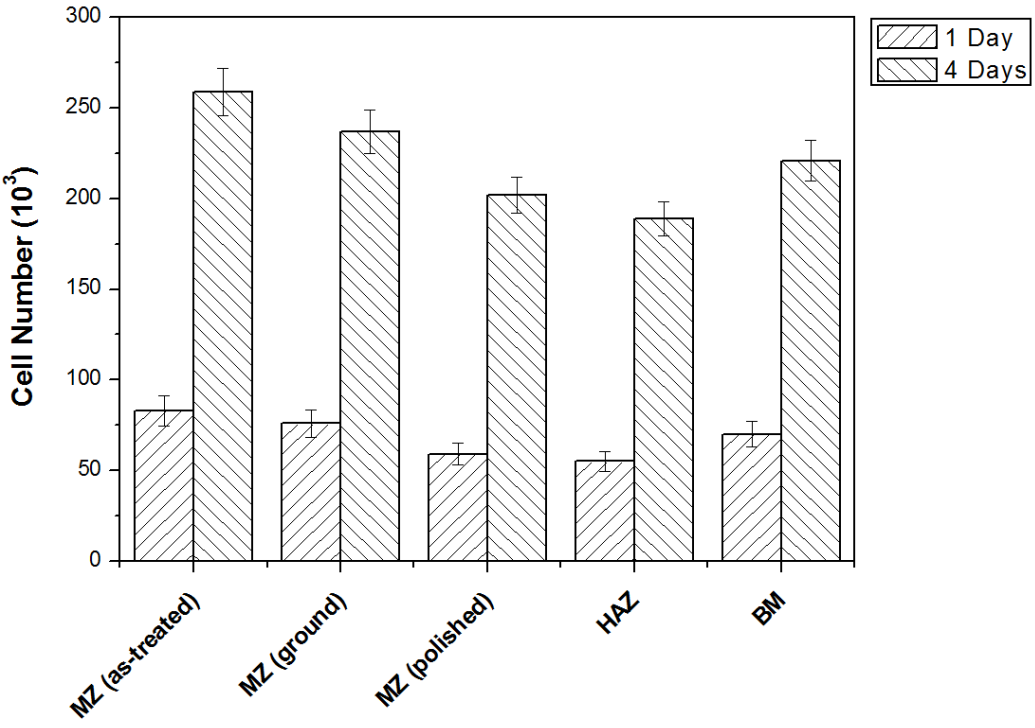

Figure 4: Number of viable MSCs cultured for 1 and 4 days on the NiTi samples.

The cell viability on different samples after 1, 4 and 7 days of culture is plotted in Fig. 8. The results in Fig. 8 show that the cell viability of MZ (as-treated) is higher than MZ (polished), HAZ and BM for all culture periods and the differences are statistically significant. MZ (as-treated) shows a significantly higher cell viability than MZ (ground) cultured for 7 days. The cell viability of MZ (ground) and BM is both significantly higher the HAZ for all culture periods and MZ (polished) cultured for 4 and 7 days. To sum up the results in the cell count and viability measurements, MZ (as-treated) shows the best biocompatibility as evidenced by the highest cell number and viability, followed by MZ (ground) or BM, with MZ (polished) or HAZ being the least.

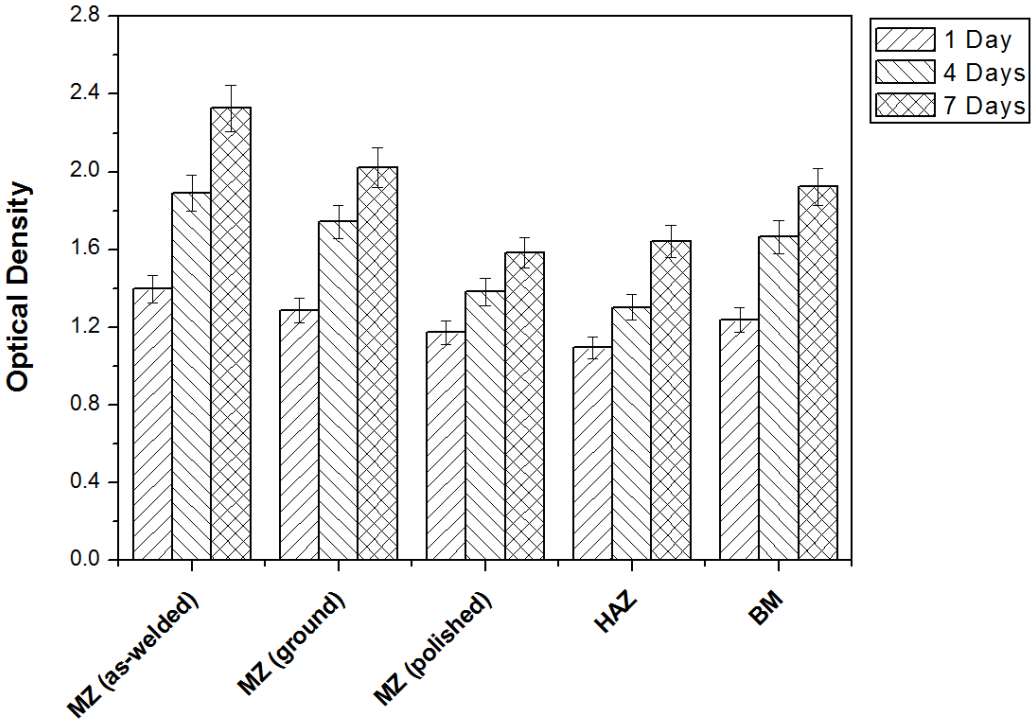

Figure 5: Viability of MSCs cultured for 1, 4 and 7 days on the NiTi samples.

Based on the above reasons, the highest cell attachment and viability measured in MZ (as-treated) can be attributed to the synergistic effect of the highest surface roughness, lowest surface Ni/TiO2 ratio, and presence of the anisotropic dendritic pattern. However, the effect of laser-induced surface features on the wetting behaviour is still inconclusive. An ongoing study in the wetting behaviour of laser-treated surface on the cell responses is being conducted in line with this research. It is important to note that the cells were cultured at 37 °C which is well above the austenite finish temperatures of all the samples. Therefore, the samples were in pure austenite phase throughout the study and the effect of phase switching on the cell attachment and viability can be neglected. On the other hand, the findings in this study are in good agreement with literature results that the rougher samples: MZ (as-treated), MZ (ground), and BM, show higher cell attachment and viability than that of the smoother sample: MZ (polished).

It is of particular interest to note that the HAZ has moderately high roughness and low surface Ni/TiO2 ratio, but the cell attachment and viability is comparable to MZ (polished) which has a smooth surface and high surface Ni/TiO2. This is most likely a result of the microstructural defects present in the oxide layer and grain structure of the HAZ. First, heat conduction through NiTi during laser treatment removes the effect of prior thermo-mechanical history and results in re-crystallization in the HAZ, analogous to the heat-treatment process between 600 and 800 °C. The heat-treatment of NiTi in such temperature range leads to the formation of a defective and porous black oxide layer which promotes the outward Ni diffusion. Defects such as voids or vacancies provide pathways for metallic Ni to diffuse from the nickel-rich underneath layers to the surface and thereby leak to the cell culture medium causing harmful effects to the cells. On the contrary, the oxide formed on the laser-melded surface was clean and compact. Such results indicate that the quality and compactness of oxide layer should be considered together with the Ni/TiO2 ratio when determining the degree of safety for NiTi implants. Second, the cell attachment was reported to be grain-size dependent. Finer grains are more favourable for the cell attachment than the coarser grains. Therefore, the defective and porous oxide layer as well as the coarse grained structure might attribute to the inferior cell attachment and viability on the HAZ compared with the BM which has similar surface morphology.

3.3.3 Comparison Between the Bioactivity of Polyamide and NiTi

Following 24 hours and 96 hour incubation times, it was found that for both the polyamide and NiTi laser surface treated samples the stem cell number count had increased significantly compared to the respective as-received materials, AR and BM. This result highlights the potential of laser surface treatment of polymers and alloys for the enhancement of stem cell growth. What is more, viability tests showed that the number of viable stem cells on the laser surface treated samples, following the two incubation times, was higher when compared to the respective as-received materials.

From the materials characterisation it was identified that there was a large increase in surface roughness and an increase in surface oxygen content – both of which are known to have an impact upon the biomimetic properties of material surfaces [3, 16-19]. These could be the main drivers which govern the stem cell reaction to the laser surface treated surfaces; however, more research is needed to verify this particular hypothesis.

4. Conclusions

Laser-induced surface treatment of polyamide and NiTi alloy and the effects on the attachment and viability of mesenchymal stem cells (MSCs), following 24 and 96 hour incubation times, has been investigated. For all laser surface treated samples, the surface roughness increased compared to the as-received samples. The polyamide samples showed a slight increase in surface oxygen content, in addition to the promotion of other potential functional groups which may have affected the stem cell growth. With regards to the NiTi alloy, the passive films at different regions of the weldment were mainly composed of TiO_2, and showed a higher surface atomic Ti/Ni ratio which is a likely parameter to have affected stem cell growth.

For the polyamide samples it was found that all samples gave rise to an increase in viable stem cell count number compared to the as-received sample (AR); whereas, for the NiTi alloy, the melt zone (MZ) showed the highest cell attachment and viability compared with the heat affected zone (HAZ) and as-received base material (BM). It is believed that this is due to the increase in surface roughness and surface oxygen content of the samples; however, it has not been ascertained which is the main driving parameter governing the biomimetic nature. In order for the biomimetic governing parameter to be identified more research is required.

5. References

[1] Mao CZ, W.; Zhu, C.; Zhu A.; Shen, J.; Lin, S. In vitro studies of platelet adhesion on UV radiation-treated nylon surface. Carbohydr Polym. 2005;59:19-25.
[2] Karaca EHAS. Analysis of the fracture morphology of polyamide, polyester, polypropylene, and silk sutures before and after implantation in vivo. J Biomed Mater Res, Part B. 2008;87B:580-9.
[3] M. Makropoulou AAS, C.D. Skordoulis. Ultra-violet and Infra-red Laser Ablation Studies of Biocompatible Polymers. Lasers in Medical Science. 1995;10:201-6.
[4] Trigwell SH, R.D.; Nelson, K.F.; Selvaduray, G. Effects of surface treatment on the surface chemistry of NiTi alloy for biomedical applications. Surface and Interface Analysis. 1998;26:483-9.
[5] Xuanyong LC, P.K.; Chuanxian, D. Surface modification of titanium, titanium alloys, and related materials for biomedical applications. Materials Science and Engineering: R: Reports. 2004;47:49-121.
[6] Bansiddhi AS, T.D.; Stupp, S.I.; Dunand, D.C. Porous NiTi for bone implants: A review. Acta Biomaterialia. 2008;4:773-82.
[7] Duerig TP, A.; Stockel, D. An overview of Nitinol medical applications. Materials Science and Engineering A. 1999;273-275:149-60.
[8] Morgan NB. Medical shape memory alloy applications - the market and its products. Materials Science and Engineering A. 2004;378:16-23.
[9] Jiangnan LS, B.; Xue, J.; Yan, S.; Zhao, W.; Folkard, M.; Michael, B.D.; Wang, Y. Study on hydrophilicity of polymer surfaces improved by plasma treatment. Applied Surface Science. 2006;252:3375-9.

[10] W. GHSAT. aser welding of NiTi wires. Materials Science and Engineering A. 2008;481-482:668-71.
[11] A.S.G. Curtis CDWW. Reactions of cells to topography. J Biomater Sci Polym Edn. 1998;9:1313-29.
[12] C. Wirth VC, C. Lagneau, P. Exbrayat, M. Lissac, N. Jaffrezic-Renault, L. Ponsonnet. Nitinol surface roughness moduluates in vitro cell responses: a comparison between fibroblasts and osteoblasts. Mater Sci Eng 2005;25:51-60.
[13] TP Kunzler CH, T. Drobek, J. Voros, N.D. Spencer. Systematic study of osteoblast response to nanotopography by means of nanoparticle-density gradients. Biomater. 2007;28:5000-6.
[14] D.S. Kommireddy SMS, Y.M. Lvov, D.K. Mills. Stem cell attachment to layer-by-layer assembled TiO2 nanoparticle thin films. Biomater. 2006;27:4296-303.
[15] S. Myllymaa EK, K. Myllymaa, T. Sillat, H. Korhonen, R. Lappalainen, Y.T. Konttinen. Adhesion, spreading and osteogenic differentiation of mesenchymal stem cells cultured on micropatterned amorphous diamond, titanium, tantalum, and chromium coatings on silicon. J Mater Sci Mater Med. 2010;21:329-41.
[16] Hao LL, J. Laser Surface Treatment of Bio-Implant Materials. New Jersey, USA: John Wiley & Sons Inc.; 2005.
[17] Waugh DG, Lawrence J. Wettability and osteoblast cell response modulation through UV laser processing of nylon 6,6. Applied Surface Science. 2011;257:8798-812.
[18] Waugh DG, Lawrence J, Morgan DJ, Thomas CL. Interaction of CO2 laser-modified nylon with osteoblast cells in relation to wettability. Material Science and Engineering C. 2009;29:2514-24.
[19] Man CWCIHDGWJLHC. Effect of Laser Treatment on the Attachment and Viability of Mesenchymal Stem Cell Responses on Shape Memory NiTi Alloy. Materials Science and Engineering C. 2014;42:254-63.